

Simultaneous Ordering of Holes and Spins in $\text{La}_2\text{NiO}_{4.125}$

J. M. Tranquada,¹ D. J. Buttrey,² V. Sachan,² and J. E. Lorenzo¹

¹*Physics Department, Brookhaven National Laboratory, Upton, New York 11973*

²*Department of Chemical Engineering, University of Delaware, Newark, Delaware 19716*
(Received 13 December 1993)

We report a single-crystal neutron diffraction study of the incommensurate magnetic ordering that occurs in $\text{La}_2\text{NiO}_{4.125}$ below 110 K. Besides the magnetic first and third harmonic Bragg peaks, we have also observed second harmonic peaks associated with charge ordering. The magnitude of the incommensurate splitting, ϵ , is strongly temperature dependent. Lock-in behavior indicates that ϵ tends to rational fractions, while regions of continuous variation suggest a devil's staircase. Analysis of these features indicates that the holes, induced by the excess oxygen, order in domain walls that form antiphase boundaries between antiferromagnetic domains.

PACS numbers: 71.27.+a, 71.38.+i, 75.50.Ee

The nature of the normal state of copper oxide superconductors such as $\text{La}_{2-x}(\text{Sr}, \text{Ba})_x\text{CuO}_{4+\delta}$ [1] continues to be a subject of controversy. Descriptions of it range from a simple Fermi liquid picture to one in which highly correlated electrons or holes move in an antiferromagnetic background of Cu spins. This debate has motivated studies on the isomorphous system $\text{La}_{2-x}\text{Sr}_x\text{NiO}_{4+\delta}$. In contrast to the cuprate system, the nickelate remains insulating except at very high Sr concentrations [2]. In this Letter we present evidence for simultaneous ordering of charges and spins in $\text{La}_2\text{NiO}_{4.125}$, which helps to explain the insulating behavior and suggests the occurrence of similar, but dynamical, correlations in the cuprates.

Band structure calculations utilizing the local-spin-density approximation would predict that doped La_2NiO_4 should be a diamagnetic metal. By explicitly taking into account on-site Coulomb interactions between Ni 3d electrons, Anisimov *et al.* [3] have calculated a ground state in which doped holes form small polarons in an antiferromagnetic background. Experimental evidence for small polarons has been found in midinfrared [4] and x-ray [5] absorption measurements in $\text{La}_{2-x}\text{Sr}_x\text{NiO}_{4+\delta}$. A neutron scattering study [6] on a crystal with $x = 0.2$ and $\delta < 0$ revealed incommensurate magnetic correlations in the NiO_2 planes that appear to freeze in below ~ 100 K. More recently, in an electron-diffraction study of ceramic samples, superlattice peaks were observed below ~ 220 K, indicating a structural modulation of the planes that varies with x [7]. A connection with the magnetic correlations has been suggested but not firmly established [7]. In contrast, the antiferromagnetic spin structure in oxygen-doped $\text{La}_2\text{NiO}_{4+\delta}$ shows remarkably little change for $0 \leq \delta \leq 11$, although the Néel temperature decreases from 335 K to 50 K [8–10].

In this paper we present the results of a neutron scattering study on a single crystal of $\text{La}_2\text{NiO}_{4+\delta}$ with $\delta = 0.125$. Yamada *et al.* [11] have shown recently that in $\text{La}_2\text{NiO}_{4.125}$ the magnetic ordering temperature rises, rather surprisingly, to 110 K, with the magnetic peaks ap-

pearing at incommensurate positions. We show that, in addition to the magnetic first and third harmonic peaks, second harmonic peaks, associated with charge ordering, also appear below 110 K. The ordering consists of charged domain walls that form antiphase boundaries between antiferromagnetic domains, similar to the structures obtained in Hartree-Fock analyses of the 2D Hubbard model [12]. Furthermore, we demonstrate that the incommensurability, which is strongly temperature dependent, does not vary continuously, but instead tends to lock in at certain rational fractions. Analysis of the observed fractions suggests that a competition between the ordering of the hole stripes and a modulation of the lattice due to ordering of oxygen interstitials leads to a devil's staircase of ordered phases.

The ordering of the interstitial oxygens occurs near room temperature, and the associated lattice modulations are fixed throughout the range where the spin and hole ordering occurs. Our identification of superlattice peaks associated with oxygen ordering is based largely on our experience with the doping range $0.05 \leq \delta \leq 0.11$ [13]. We have learned that the unit cell doubling along the c axis that we observed for $\delta = 0.105$ [10] can be explained by a one-dimensional ordering of interstitial oxygen layers, much like the stage-2 ordering of alkali metals in graphite. (There is no need to invoke a charge-density-wave ordering, as we had done previously [10].) The Bragg-like superlattice peaks are caused by scattering from the induced tilt pattern of the NiO_6 octahedra, rather than from the interstitial oxygens themselves. For $\delta = 0.125$ we find that the interstitials actually order three dimensionally, creating a large unit cell.

The 1.3 g crystal used in our study was obtained from a boule grown congruently by rf induction skull melting [14]. The oxygen concentration was selected by annealing at 700°C in 1 atm O_2 for several hours, followed by a quench to room temperature. The value of δ was checked by iodometric analysis of other material prepared in the same anneal. The neutron diffraction measurements were

performed on the H4M and H8 triple-axis spectrometers at the High Flux Beam Reactor at Brookhaven National Laboratory. The (002) reflection of pyrolytic graphite (PG) was used for the monochromator and analyzer, together with a PG filter in the incident beam to eliminate $\lambda/2$ contamination. Measurements were performed with 14.7 meV neutrons, and the crystal was cooled with a Displex closed-cycle He refrigerator.

To describe the diffraction peaks, we will use an indexing based on an orthorhombic cell (with the c axis perpendicular to the planes) of $\sqrt{2} \times \sqrt{2} \times 1$ relative to the basic body-centered tetragonal cell. While the fundamental reflections indicate a tetragonal symmetry down to low temperature, with $a = 5.457 \text{ \AA}$ and $c = 12.62 \text{ \AA}$ at 10 K, the structural superlattice peaks suggest an orthorhombic symmetry. The crystal was initially oriented in the $(h0l)$ zone; however, twinning causes the simultaneous presence of $(0kl)$ reflections. We have also studied the superlattice reflections in the $(hk0)$ zone. The lack of a difference between \mathbf{a}^* and \mathbf{b}^* prevents a unique indexing of the observed reflections. We therefore make a somewhat arbitrary assignment, the justification for which should become clear shortly. The types of superlattice peaks that we have observed are listed in Table I.

There are basically two types of superlattice peaks associated with the oxygen ordering, one involving a modulation of period $3a$, and the other with a period of $5b \times 5c$. The temperature dependence of the intensity of one peak of each type is shown in Fig. 1. The sample was initially cooled rapidly from room temperature to 10 K, where the measurements began. The intensities remained fairly constant on warming to 200 K, but increased at 250 K before dropping toward zero near 310 K. On subsequent slow cooling to 210 K, significant time dependence of the intensities was observed while sitting at a given temperature. Below 200 K the intensities do not change. The behavior seen here is consistent with observations of oxygen ordering in crystals with $\delta \leq 0.11$ [13], with the exception that the ordering is now three dimensional. The identical temperature dependences of the two types of reflections shows that both are associated with a single

ordering transition. Phase separation is ruled out by the dramatic crossover observed in the magnetic ordering as a function of δ , from commensurate at $\delta = 0.105$ [10] to incommensurate at $\delta = 0.116$ [13]. We expect that, as for $\delta \leq 0.11$, the atomic displacements associated with the interstitial order involves tilts of the NiO_6 octahedra; the distortions of the NiO_2 planes, where the magnetism occurs, should be small.

The magnetic ordering transition at 110 K was first detected by magnetization measurements [11]. Neutron diffraction measurements showed that the magnetic structure is incommensurate, and both first and third harmonic peaks of the types listed in Table I were observed [11]. The peaks are split about the commensurate antiferromagnetic positions by an amount $n\epsilon$ ($n = 1, 3$), where $\epsilon \approx 0.275$ at low temperature. In our own neutron diffraction study we have discovered second harmonic peaks split about a different set of wave vectors (see Table I). Structure factors $|F_{n\epsilon}|$ for the three harmonics, extracted from integrated intensity measurements for $(h0l)$ reflections, are plotted as a function of momentum transfer Q in Fig. 2(a). In contrast to $|F_\epsilon|$ and $|F_{3\epsilon}|$, which fall off like the Ni magnetic form factor, $|F_{2\epsilon}|$ increases with Q , indicating that the second harmonic is associated with a structural, rather than magnetic, modulation in the planes. The combination of the incommensurate antiferromagnetic splitting ϵ with a strain wave at 2ϵ is similar to what is found in Cr [15].

What causes the strain wave? A likely explanation is the ordering of the doped holes, which would cause a modulation of Ni-O bond lengths within the planes. If each excess oxygen dopes two holes into the planes, then at $\delta = 0.125$ there should be 1 hole/4 Ni. A 1D ordering of the holes into stripes, as indicated in Fig. 2(b), results in a modulation with period of $2a$. Furthermore, if the hole stripes act as antiphase domain boundaries, then the antiferromagnetic period is $4a$. This is exactly the type of structure that has been found in Hartree-Fock analyses of the Hubbard model [12]. We have also considered a model involving a spiraling of the Ni spins as they cross the charged domain walls; however, an analysis of intensities for 17 first harmonic peaks measured in the

TABLE I. Types of superlattice reflections observed in the $(h0l)$, $(0kl)$, and $(hk0)$ zones of $\text{La}_2\text{NiO}_{4.125}$.

Ordered entity	Coordinates	Conditions			
		h	k	l	
Interstitial	$(h \pm \frac{1}{3}, 0, l)$	even		odd	
Oxygens	$(h \pm \frac{1}{3}, k, 0)$	odd	odd		
	$(h \pm \frac{2}{3}, k, 0)$	even	even		
Spins	$(0, k \pm \frac{2}{5}n, l \pm \frac{2}{5}n)$		even	even	$n = 1, 2$
	$(h \pm n\epsilon, k, l)$	odd	even	integer	$n = 1, 3$
	$(h \pm n\epsilon, k, 0)$	even	odd		$n = 1, 3$
Holes	$(h \pm 2\epsilon, 0, l)$	even		odd	
	$(h \pm 2\epsilon, k, 0)$	odd	odd		

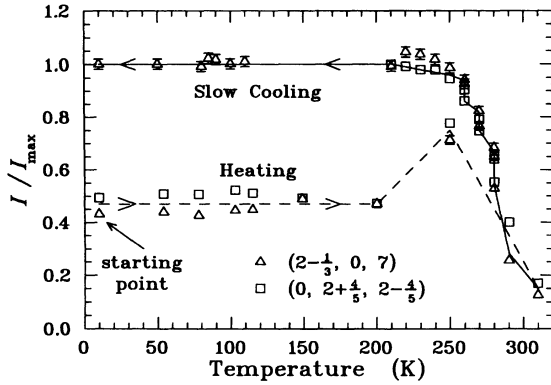


FIG. 1. Temperature dependence of the relative intensities of two oxygen-ordering superlattice peaks observed following an initial rapid cooling of the sample to 10 K. The lines and arrows indicate the order in which the measurements were made.

(*hk*0) zone indicates that the spin pattern shown in Fig. 2(b) is essentially correct. The *l* dependence of the 2ϵ peak intensities indicates that the pattern is displaced by the vector $\mathbf{a} + \frac{1}{2}\mathbf{b} + \frac{1}{2}\mathbf{c}$ in going from one plane to the next, consistent with Coulomb repulsion between hole stripes in neighboring planes.

One small problem with the proposed spin structure is that it predicts ϵ to be exactly $\frac{1}{4}$. The observed ϵ differs slightly from this value, and actually exhibits a substantial temperature dependence, as shown in Fig. 3. A close inspection suggests that near 80 K and 60 K the ϵ determined by the peak intensity maximum (rather than peak center) tends to plateau at the rational fractions $\frac{5}{18}$ and $\frac{3}{11}$, respectively. The peak intensity resonates in the same temperature regions. The difference in

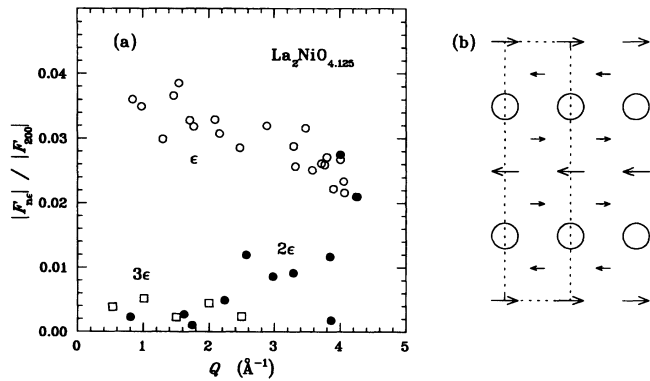


FIG. 2. (a) Measured structure factors $|F_{n\epsilon}|$ of the ϵ , 2ϵ , and 3ϵ peaks, normalized to the value for the fundamental (200) peak. Data obtained from integrated intensities for peaks in the (*h*0*l*) zone measured at 10 K. Note that intensity is proportional to $|F|^2$. (b) Model of spin and hole ordering in a NiO_2 plane, as discussed in the text; circles indicate positions of holes (each centered on a Ni and shared by 4 O neighbors), arrows indicate Ni spins, and the dotted line indicates the unit cell size.

behavior relative to the integrated intensity is due to width variations, which suggest the presence of multiple peak components at a given temperature.

To resolve the different components, we must look at the third harmonic peaks. Scans through the $(1 - 3\epsilon, 0, 1)$ peaks at various temperatures are shown in Fig. 4. A resolution-limited peak appears at $1 - 3\epsilon = \frac{1}{6}$ ($\epsilon = \frac{5}{18}$) at 85 K, increasing in intensity at 75 K, and then decreasing somewhat at lower temperatures. At 60 K, a peak appears at $1 - 3\epsilon = \frac{2}{11}$ ($\epsilon = \frac{3}{11}$) with a width 3 times that of the $\frac{1}{6}$ peak. These measurements clearly define the rational fractions associated with the major plateaus in ϵ .

The observed rational fractions can be expressed in the form

$$\epsilon = \frac{n + m}{4n + 3m}, \quad (1)$$

where *n* and *m* are non-negative integers. For *m* = 0, we obtain the ideal fraction of $\frac{1}{4}$, while for *n* = 0 we get $\frac{1}{3}$. The fractions $\frac{3}{11}$ and $\frac{5}{18}$ correspond to *n* = 2,

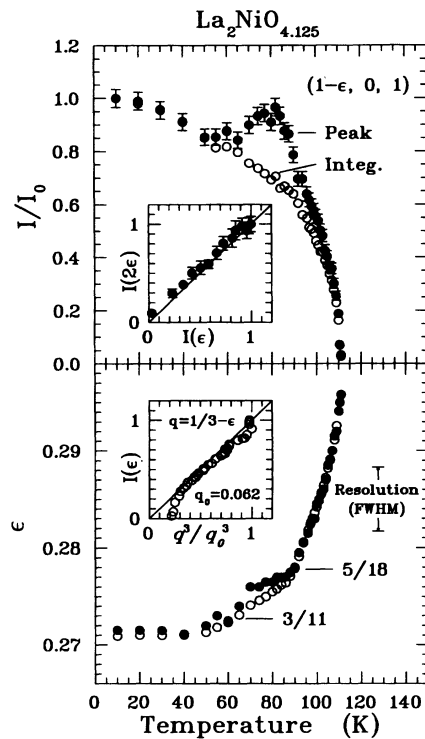


FIG. 3. Upper panel: Temperature dependence of the relative intensity of the magnetic $(1 - \epsilon, 0, 1)$ peak; integrated intensity (solid circles), and peak intensity (open). Inset: Relative intensity of the structural second harmonic peak at $(4 - 2\epsilon, 0, 1)$, with temperature as an implicit parameter. Lower panel: Temperature dependence of ϵ measured at $(1 - \epsilon, 0, 1)$; ϵ corresponds to the peak maximum position (solid circles) and the average position (open circles). Inset: Relative intensity of the $(1 - \epsilon, 0, 1)$ peak vs $(q/q_0)^3$, where $q = \frac{1}{3} - \epsilon$ and $q_0 = 0.062$; temperature is an implicit variable.

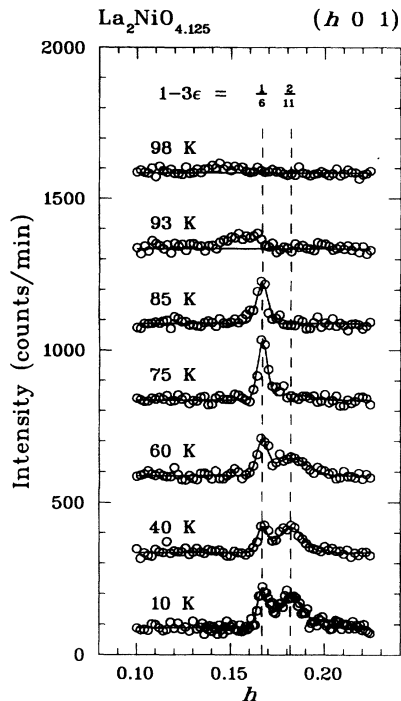


FIG. 4. Scans along $(h01)$ through the magnetic $(1 - 3\epsilon, 0, 1)$ peaks at various temperatures. The intensity scale is correct for the 10 K scan; the others have been offset vertically.

$m = 1$ and $n = 3$, $m = 2$, respectively. In terms of the spin structure, the rational fractions indicate that the spin modulation must complete $n + m$ periods in a unit cell of length $(4n + 3m)a$. If all combinations of n and m are allowed, then the resulting values of ϵ describe a devil's staircase. Some form of pinning presumably makes certain values of ϵ more favorable than others. We suggest that the occurrence of the rational fractions is the result of a competition between two length scales, one associated with the ideal spin-charge order $(4a)$, and the other associated with modulation of the lattice potential due to ordering of the oxygen interstitials $(3a)$.

It is interesting to consider the order parameter for the phase transition. As shown in the upper inset of Fig. 3, the intensity of the $(4 - 2\epsilon, 0, 1)$ peak is directly proportional to that of $(1 - \epsilon, 0, 1)$ as a function of temperature. This is quite different from Cr, where the amplitude of the spin-density wave is the primary order parameter and $I(2Q) \sim I^2(Q)$ [15]. We suggest that the order parameter in the present case is the wave vector difference $q = \frac{1}{3} - \epsilon$. As shown in the lower inset of Fig. 3, we find that $I(\epsilon) \sim q^3$ over most of the temperature range below the transition.

The simultaneous ordering of spins and charges is also observed in new measurements (to be reported elsewhere [16]) on a crystal of $\text{La}_{1.8}\text{Sr}_{0.2}\text{NiO}_{4.00}$ with stoichiometric oxygen content. In that case, the correlation length for the ordering is finite, but $\epsilon = \frac{1}{4}$. The observed ordering of spins and charges in the nickelates is a form of

microscopic, electronic phase separation that is presumably stabilized by electron-phonon interactions. Emery and Kivelson [17] have suggested that a dynamic electronic phase separation could be a crucial component of the superconducting mechanism in the cuprates. Could it be that charged domain walls forming magnetic antiphase boundaries exist in $\text{La}_{2-x}\text{Sr}_x\text{CuO}_4$, but fail to order due to quantum fluctuations associated with the smaller magnetic moments? Such possibilities will be tested in future experiments.

We are indebted to K. Yamada for sharing his results prior to publication, and gratefully acknowledge valuable discussions with J.D. Axe, V.J. Emery, G. Shirane, and B.J. Sternlieb. Work at Brookhaven was carried out under Contract No. DE-AC02-76CH00016, Division of Materials Sciences, U.S. Department of Energy. D.J.B. and V.S. acknowledge support from the National Science Foundation under Contract No. DMR-8914080.

- [1] J.G. Bednorz and K.A. Müller, *Z. Phys. B* **64**, 189 (1986).
- [2] R.J. Cava, B. Batlogg, T.T. Palstra, J.J. Krajewski, W.F. Peck, Jr., A.P. Ramirez, and L.W. Rupp, Jr., *Phys. Rev. B* **43**, 1229 (1991), and references therein.
- [3] V.I. Anisimov, M.A. Korotin, J. Zaanen, and O.K. Andersen, *Phys. Rev. Lett.* **68**, 345 (1992).
- [4] X-X. Bi and P.C. Eklund, *Phys. Rev. Lett.* **70**, 2625 (1993).
- [5] P. Kuiper, D.E. Rice, D.J. Buttrey, L.H. Tjeng, and C.T. Chen (unpublished).
- [6] S.M. Hayden, G.H. Lander, J. Zaretsky, P.J. Brown, C. Stassis, P. Metcalf, and J.M. Honig, *Phys. Rev. Lett.* **68**, 1061 (1992).
- [7] C.H. Chen, S-W. Cheong, and A.S. Cooper, *Phys. Rev. Lett.* **71**, 2461 (1993).
- [8] G. Aeppli and D.J. Buttrey, *Phys. Rev. Lett.* **61**, 203 (1988); T. Freltoft, D.J. Buttrey, G. Aeppli, D. Vaknin, and G. Shirane, *Phys. Rev. B* **44**, 5046 (1991).
- [9] S. Hosoya, T. Omata, K. Nakajima, K. Yamada, and Y. Endoh, *Physica (Amsterdam)* **202C**, 188 (1992).
- [10] J.M. Tranquada, D.J. Buttrey, and D.E. Rice, *Phys. Rev. Lett.* **70**, 445 (1993).
- [11] K. Yamada, T. Omata, K. Nakajima, Y. Endoh, and S. Hosoya, *Physica (Amsterdam)* **221C**, 355 (1994).
- [12] D. Poilblanc and T.M. Rice, *Phys. Rev. B* **39**, 9749 (1989); J. Zaanen and O. Gunnarsson, *ibid.* **40**, 7391 (1989); H.J. Schultz, *Phys. Rev. Lett.* **64**, 1445 (1990).
- [13] J.M. Tranquada, Y. Kong, J.E. Lorenzo, T.R. Thurston, D.J. Buttrey, D.E. Rice, and V. Sachan, *Phys. Rev. B* (to be published).
- [14] D.E. Rice and D.J. Buttrey, *J. Solid State Chem.* **105**, 197 (1993).
- [15] R. Pynn, W. Press, S.M. Shapiro, and S.A. Werner, *Phys. Rev. B* **13**, 295 (1976).
- [16] V. Sachan, D.J. Buttrey, J.M. Tranquada, J.E. Lorenzo, and G. Shirane (unpublished).
- [17] V.J. Emery and S.A. Kivelson, *Physica (Amsterdam)* **209C**, 597 (1993).